THE JOURNAL OF BIOLOGICAL CHEMISTRY VOL. 290, NO. 13, pp. 8218–8231, March 27, 2015

Basic Leucine Zipper (bZIP) Domain Transcription Factor MBZ1 Regulates Cell Wall Integrity, Spore Adherence, and Virulence in *Metarhizium robertsii*[*]

Received for publication, December 8, 2014, and in revised form, February 5, 2015 Published, JBC Papers in Press, February 10, 2015, DOI 10.1074/jbc.M114.630939

Wei Huang, Yanfang Shang, Peilin Chen, Kai Cen, and Chengshu Wang[1]

From the Key Laboratory of Insect Developmental and Evolutionary Biology, Institute of Plant Physiology and Ecology, Shanghai Institutes for Biological Sciences, Chinese Academy of Sciences, Shanghai 200032, China

Background: The bZIP-type transcription factors are widely distributed in eukaryotes to control an array of biological activities.
Results: MBZ1 from *Metarhizium robertsii* regulates fungal growth, cell wall integrity, spore adherence, and virulence against insects.
Conclusion: MBZ1 is required for development and virulence of insect pathogenic fungi.
Significance: The orthologs of bZIP-type transcription factors are functionally divergent in different organisms.

Transcription factors (TFs) containing the basic leucine zipper (bZIP) domain are widely distributed in eukaryotes and display an array of distinct functions. In this study, a bZIP-type TF gene (*MBZ1*) was deleted and functionally characterized in the insect pathogenic fungus *Metarhizium robertsii*. The deletion mutant (Δ*MBZ1*) showed defects in cell wall integrity, adhesion to hydrophobic surfaces, and topical infection of insects. Relative to the WT, Δ*MBZ1* was also impaired in growth and conidiogenesis. Examination of putative target gene expression indicated that the genes involved in chitin biosynthesis were differentially transcribed in Δ*MBZ1* compared with the WT, which led to the accumulation of a higher level of chitin in mutant cell walls. MBZ1 exhibited negative regulation of subtilisin proteases, but positive control of an adhesin gene, which is consistent with the observation of effects on cell autolysis and a reduction in spore adherence to hydrophobic surfaces in Δ*MBZ1*. Promoter binding assays indicated that MBZ1 can bind to different target genes and suggested the possibility of heterodimer formation to increase the diversity of the MBZ1 regulatory network. The results of this study advance our understanding of the divergence of bZIP-type TFs at both intra- and interspecific levels.

Much of our knowledge about the features and functions of transcription factors (TFs),[2] including a group of structurally and functionally related members containing the conserved basic leucine zipper (bZIP) domain, comes from the discovery and study of AP-1 (activating protein 1) (1). The bZIP TFs are one of the largest families of dimerizing TFs and are widely distributed in the genomes of all eukaryotes (2). The prototypical bZIP TF was first discovered over 30 years ago in humans (3), and members are now classified into 19 families regulating a plethora of biological functions, including the cell cycle, development, reproduction, metabolism, and programmed cell death (2). Besides animals, bZIP-type TFs have also been well characterized in plants by mediating pathogen defense, abiotic stress response, hormone signaling, energy metabolism, and senescence (4).

In fungi, a bZIP-type TF was first characterized as YAP1 (yeast activating protein 1) in *Saccharomyces cerevisiae* (5), and then members of the family (YAP1–YAP8) were found and verified to be functionally distinct in yeast (6). Different bZIP-type TFs have also been characterized in various filamentous fungal species, including *Aspergillus nidulans* (7, 8), *Neurospora crassa* (9), and the plant pathogens *Fusarium graminearum* (10–12) and *Magnaporthe oryzae* (13–15). Deletions and functional characterizations of these genes revealed that bZIP-type TFs are involved in mediating fungal development, sexuality, stress responses, secondary metabolisms, and especially the virulence of plant pathogens. For example, the bZIP-type TF FGZIF1 was identified to be involved in the control of mycotoxin deoxynivalenol production, sexuality, and virulence in *F. graminearum* (11). MOAP1 of *M. oryzae* was functionally verified as a positive regulator of different target genes involved in growth, development, and pathogenicity (14). Genome analyses of insect fungal pathogens such as *Metarhizium robertsii* (16), *Cordyceps militaris* (17), and *Beauveria bassiana* (18) also identified an array of bZIP-type TFs present in their genomes. However, none of these has been functionally studied.

Insect pathogenic fungi such as *M. robertsii*, *Metarhizium acridum*, and *B. bassiana* diverged after mammalian and plant pathogens (19) and have been developed as promising and environmentally friendly mycoinsecticides (20, 21). Molecular pathogenesis studies have revealed the functions of genes involved in insect cuticle adherence, degradation, penetration, immune invasion, and production of insecticidal mycotoxins (22, 23). However, the TFs involved in regulation of virulence-related genes are still unknown.

* This work was supported by National Natural Science Foundation of China Grant 31225023 and Chinese Academy of Sciences Strategic Priority Research Program Grant XDB11030100.
[1] To whom correspondence should be addressed. Tel.: 86-21-5492-4157; Fax: 86-21-5492-4015; E-mail: cswang@sibs.ac.cn.
[2] The abbreviations used are: TF, transcription factor; bZIP, basic leucine zipper; PDA, potato dextrose agar; SDB, Sabouraud dextrose broth; Comp, complemented mutant; LT_{50}, median lethal time; qRT-PCR, quantitative real-time PCR; CREB, cAMP response element-binding protein.

In this study, the bZIP-type TF gene MAA_01736, designated *MBZ1*, was deleted and functionally characterized in the insect pathogen *M. robertsii.* This gene was previously found to be highly transcribed by the fungus during early infection (16). Our functional studies showed that *MBZ1* mediates both positive and negative regulation of different target genes involved in growth, sporulation, cell wall integrity, spore adherence, and virulence against insect hosts in *M. robertsii*.

EXPERIMENTAL PROCEDURES

Fungal Strains and Culturing Conditions—The WT strain and mutants of *M. robertsii* ARSEF 2575 were routinely maintained on potato dextrose agar (PDA; Difco) or on complete mineral medium for the conidiation assays at 25 °C (24). In addition, the PDA medium was buffered with final concentrations of 1 μg/ml tunicamycin (Sigma), 200 μg/ml Calcofluor White (Sigma), 300 μg/ml amphotericin B (Biosharp), 4 mM $CuSO_4$, 0.5 M sorbitol, 1 mM DTT, or 0.01% SDS for cell well stress challenges (25, 26). For liquid incubation, fungi were grown in Sabouraud dextrose broth (SDB; Difco) with or without 50 μg/ml Congo red (Bio Basic Inc.) at 25 °C for 18 h in a rotary shaker. To induce protease expression, fungal cultures were grown in a minimum medium containing 1% silkworm pupa homogenate at 25 °C in a rotary shaker (27). For mycotoxin production assays, the WT and mutants were grown in Czapek Dox broth at 25 °C for 1 week in a rotary shaker (28). Yeast strains AH109 (*MAT***a**, *TRP1-901*, *LEU2-3,112*, *URA3-52*, *HIS3-200*, *GAL4*Δ, *GAL80*Δ, *LYS2*::$GAL1_{UAS}$-$GAL1_{TATA}$-*HIS3*, *MEL1* $GAL2_{UAS}$-$GAL2_{TATA}$-*ADE2*, *URA3*::$MEL1_{UAS}$-$MEL1_{TATA}$-*LACZ*) and EGY48 (*MATα*, *TRP1*, $HIS3^-$, $URA3^-$, *LEU2*::6 *LEX-AOPS-LEU2*) (Invitrogen) were used for yeast one-hybrid transcriptional activation tests. The yeast cells were cultured in 1% yeast extract, 2% peptone, 2% glucose, and 2 mg/liter adenine; 1% yeast extract, 2% peptone, and 2% glucose; or synthetic dropout medium (24, 29).

Bioinformatics Analysis—Genome-wide surveys for bZIP domain-containing TFs were performed by BLASTp searches of the genomes of *M. robertsii* and other fungi. The protein sequences of functionally verified bZIP-type TFs from yeast and other species were found and aligned with those from *M. robertsii* with ClustalX 2.0 (30). A maximum likelihood tree was generated using a Dayhoff model with 1000 replicates for bootstrapping using the program MEGA6 (31). For analysis of the putative MBZ1-binding site, the promoter regions (~1.5 kb upstream of each start codon) of selected genes were retrieved and analyzed using the weight matrix-based program Match (version 1.0).

Subcellular Localization and Transcriptional Activation Assays—For the subcellular localization assay of MBZ1, the *HSP70* gene (MAA_02081) promoter, *GFP*, and full-length *MBZ1* genes were amplified individually by PCR, and the cassette was generated by fusion PCR with different primer pairs (Table 1). The product was cloned into binary vector pDHT-BAR to produce plasmid pBAR-HSP70p-GFP-linker-MBZ1 with a ClonExpress kit (Vazyme). The resulting vector was used for transformation of the *M. robertsii* strain. For the transcriptional activation test, full-length cDNA of *MBZ1* was amplified from a cDNA library with primers 1736CF and 1736CR and cloned into the NdeI and BamHI sites of the yeast vector pBKT7 (Invitrogen) under the control of the *GAL4* promoter to generate plasmid pBKT7-MBZ1 for transformation into the AH109 yeast strain. Putative prototrophic transformants were selected using a Trp-free synthetic dropout medium and further transferred into Trp/His/Ade-free synthetic dropout plates for transcriptional activation assays. The negative control was made by transforming yeast with the blank vector, and the positive control yeast was transformed with the pBKT7 vector containing the GAL4 activation domain sequence (29).

Gene Deletion and Complementation—Targeted gene deletion of the *MBZ1* gene was performed by homologous recombination via *Agrobacterium*-mediated fungal transformation as described previously (32, 33). In brief, the 5′- and 3′-flanking sequences were amplified using the genomic DNA as a template with primer pairs TF1736UF/TF1736UR and TF1736DF/TF1736DR, respectively (Table 1). The respective products were digested with the restriction enzymes EcoRI, XhoI, and XbaI and then inserted into the corresponding sites of the binary vector pDHT-BAR (conferring ammonium glufosinate resistance) to produce plasmid pBAR-MBZ1-KO for fungal transformation. For null mutant complementation, the ORF of the *MBZ1* gene was amplified with its promoter and terminator regions using primer pairs 1736SF and 1736SR. The product was digested with XbaI and then inserted into vector pDHT-BEN to generate pBEN-MBZ1 (conferring resistance to benomyl) (34). The mutants were verified by PCR and RT-PCR analyses with primers TF1736F and TF1736R (Table 1). The complemented mutant was designated Comp.

Extraction and Quantification of Cell Wall Chitin—To quantify the chitin component of fungal cell walls, mycelia were harvested from SDB cultures; washed twice with sterile-distilled water; ground in liquid nitrogen; extracted with buffer containing 50 mM Tris-HCl (pH 7.8), 2% SDS, 0.3 M β-mercaptoethanol, and 1 mM EDTA; and incubated at 100 °C for 15 min. After centrifugation at 8000 × *g*, the pellet was washed three times with water and completely dried. The samples were dissolved in water to make a solution of 25 mg/ml. In total, 5 mg each of cell wall samples were acidified in 6 M HCl at 100 °C for 4 h. Quantification of chitin was conducted by measuring the acid-released glucosamine from chitin using the substrate *p*-dimethylaminobenzaldehyde as a chromogen (35). The absorbance was measured at 520 nm using a BioPhotometer (Eppendorf), and the quantity of glucosamine was calculated in reference to the standard curve established using pure glucosamine (Sigma) (36).

Lectin Binding Assays—To further examine fungal cell well integrity, fungal germlings of the WT and mutants were treated with different fluorescent lectins, including Alexa Fluor 488-labeled concanavalin A (60 μg/ml) for binding α-mannopyranosyl and α-glucopyranosyl residues, lectin II isolated from the legume *Griffonia simplicifolia* (20 μg/ml; Invitrogen) for binding α- or β-linked GlcNAc, and fluorescein-labeled *Galanthus nivalis* lectin (20 μg/ml; Vector Labs) for binding α-1,3-mannose (25). Images were taken with a BX51-33P fluorescence microscope (Olympus).

Conidial Adhesion and Hydrophobicity Assays—Quantitative adhesion assays were conducted by labeling the fungal spores with FITC and incubating the microtiter plates in the

TABLE 1
Oligonucleotide primers used in this study

Primer	Sequence (5′ to 3′)	Usage
TF1736DF	GCTCTAGAACTCCGTACAGCCACAATCC	For construction of gene disruption vector pBAR-MBZ1
TF1736DR	GCTCTAGATCAGTGTCTGGGTCGTTGAG	
TF1736UF	GGAATTCCCCAAGGACATTGACACAGA	
TF1736UR	CCGCTCGAGCGGTCCGACGTATTCTTGTT	
TF1736F	GCCTGTGATGGCAGTTACAA	For RT-PCR verification
TF1736R	ACACAACGGAGTCAATGCTG	
TubF	GATCTTGAACCTGGCACCAT	Used as an internal control for RT-PCR
TubR	CCATGAAGAAGTGCAGACGA	
1736SF	GCTCTAGATGGGCAGGTACGGAGTAGTT	For construction of gene complementation vector pBEN-MBZ1
1736SR	GCTCTAGAATTGGTCGAGTGGCGTAAAG	
1736CF	GGAATTCCATATGATGTCGACTTCTAGCCAAAC	For testing transcription activation
1736CR	CGGGATCCTTATATGTCCATGGTCAAAAG	
Hsp70F	CGGGCCCCCCCTCGAGGCAGTAGAGGTGTAGTTG	For generating plasmid pBAR-HSP70p-GFP-linker-MBZ1
Hsp70R	TGTGGTGGTTGTGATGCG	
1736GF	ATCACAACCACCACAATGGTGAGCAAGGGCGAGGA	
1736GR	CTTGTACAGCTCGTCCATGC	
1736CfusionF	GACGAGCTGTACAAGGGCGGAGCTGGTGCGGGCGCAGGCAT GTCGACTTCTAGCCAAAC	
1736CfusionR	CGGGCTGCAGGAATTCTTATATGTCCATGGTCAAAA	
1794F	TCATAGACACGGAACAAT	For RT-PCR and qRT-PCR analyses
1794R	GAGTAGCCGATAGGGATA	
2558F	TAGAGGTCAAAGGCAACG	
2558R	TGTGACGGCACGAAGATA	
2062F	TGGTTCCTTCCACACGTACA	
2062R	CTTGGAGAAGTCGGTGAAGC	
4636F	TACTTCCAGAGCGTCGAGGT	
4636R	AAAAACCACACCAGGCAAAG	
2408F	AGAGAAGACGTACGGTGTCG	
2408R	CTTGCACATCTTCGTCTGTG	
5675F	ACCAAGGAGGAGCTGAAGAT	
5675R	TGATACCGGAGTAGGAACCA	
10246F	CGGTCCTTCCAGATAAAC	
10246R	CAGAGTCAACTTTGTTTGGT	
10260F	ACCACCATAGCTGGATTCAA	
10260R	GAGAACCTTGACGGCATAGA	
7202F	GACGGAGACAAGAAGAACG	
7202R	AATAACAAGCGGCGAACC	
3775F	CAGGCTTCTGCTACCTTTGG	
3775R	TGTCGAAGCTGTCAATGGAG	
1736HF	GACTAGTTGTCGACTTCTAGCCAAACC	For construction of plasmid pPC86-MBZ1
1736HR	CGAGCTCTTATATGTCCATGGTCAAAA	
pPC86F	TATAACGCGTTTGGAATCACT	
pPC86R	GTAAATTTCTGGCAAGGTAGAC	
1794YF	AGTTATTACCCTCGAGCGTCCAATGCTGCAAGACTA	For generating p178-Xpromoter plasmids for yeast one-hybrid tests
1794YR	GGCGGATCTGCTCGAGATGAAATGAGGCCGTAGTGG	
2558YF	AGTTATTACCCTCGAGGGAGGGGGTTTGTTAATGT	
2558YR	GGCGGATCTGCTCGAGGTATCACCCCTGCAAATGA	
2062YF	AGTTATTACCCTCGAGTGGAGCTTCAAGTGTCATG	
2062YR	GGCGGATCTGCTCGAGGAGCGGGATATGTCAAGGA	
4636YF	AGTTATTACCCTCGAGAGCCCCCTTTTCTTTGTGTT	
4636YR	GGCGGATCTGCTCGAGACCTCGACGCTCTGGAAGTA	
2408YF	AGTTATTACCCTCGAGCAGCCAAAAGCCAAATCAAC	
2408YR	GGCGGATCTGCTCGAGGGTCTTGTTGGGCACATTCT	
5675YF	AGTTATTACCCTCGAGAGAGGGCAGGTTCAAAGACA	
5675YR	GGCGGATCTGCTCGAGGTACGGGACCAAAGACCAGA	
10246YF	AGTTATTACCCTCGAGTGTTGTAGACCCCTCCAAGG	
10246YR	GGCGGATCTGCTCGAGTTGCTGCAGGACGATGTTAG	
10260YF	AGTTATTACCCTCGAGTGGTCAGTGGTGGTCACTGT	
10260YR	GGCGGATCTGCTCGAGCTTGGTAGGAGCGAGAATCG	
7202YF	CCGCTCGAGACCCAGCCGAGTTAAGGTTT	
7202YR	CCGCTCGAGACCGCAACTGGGAATAATTG	
3775YF	AGTTATTACCCTCGAGCTGGCTGTCATGGAGTCTG	
3775YR	GGCGGATCTGCTCGAGTGGATGTCAGGCACGTAAA	

dark for 1 h (25). After removing the unbound cells, the fluorescence of each sample was measured with a Varioskan Flash microplate reader (Thermo Scientific). Variation in spore surface hydrophobicity between the WT and mutants was examined using hexadecane as described previously (26).

Insect Bioassays—Virulence tests were conducted for the WT, Δ*MBZ1*, and Comp against newly emerged last-instar larvae of silkworms (*Bombyx mori*) and wax moths (*Galleria mellonella*). Topical infections were performed by immersing insect larvae for 30 s in a spore suspension containing 1×10^7 conidia/ml. Each treatment had three replicates with 15 insects each, and the experiments were repeated three times. Mortality was recorded every 12 h. For injection assays to bypass insect cuticle barriers, each insect was injected in the second proleg with 10 μl of a spore suspension containing 1×10^6 conidia/ml. The median lethal time (LT_{50}) was calculated as described previously (34). Dead insects were removed and placed on moist filter paper in Petri dishes. To determine and compare the differences in fungal penetration processes between the WT and mutants, insect cadavers were fixed in Carnoy's solution (60%

ethanol, 30% chloroform, and 10% glacial acetic acid), dehydrated in alcohol, and embedded in paraffin wax for cutting (10 μm thick) with a rotary microtome (Leica) (32).

Appressorium Induction and Mycotoxin Quantification—To examine *MBZ1* regulation of fungal differentiation, conidia of the WT and mutants were used for infection structure induction. The hind wings from cicada (*Cryptotympana atrata*) were collected and surface-sterilized in 37% H_2O_2 for 5 min, washed twice in sterile water, and immersed in a conidial suspension (2×10^7 spores/ml) for 20 s. The inoculated wings were incubated on 0.8% water agar at 25 °C for 24 h. Appressoria were induced on a hydrophobic surface in 1% glycerol-buffered minimum medium (34). To examine whether *MBZ1* is involved in regulation of secondary metabolism, the induction, extraction, and quantification of cyclopeptide destruxins were performed as described previously (37).

Protease Activity Assay and Western Blotting—For protease activity assays, conidia of the WT, Δ*MBZ1*, and Comp were inoculated in SDB at a final concentration of 10^6 conidia/ml and incubated at 25 °C for 48 h at 180 rpm. The mycelia were then washed twice with sterile-distilled water, transferred to a basal salt medium supplemented with 1% (w/v) homogenized silkworm pupae, and incubated at 25 °C for 48 h at 180 rpm (27). The alkaline protease activities were assayed using the substrate *N*-succinyl-Ala_2-Pro-Phe *p*-nitroanilide (Sigma) as described previously (38). The protein concentration of each sample was determined using the Bradford method (34). All experiments were repeated twice, and each sample had three replicates. To confirm protease expression, Western blot analysis was conducted using an antibody against *Metarhizium* protease PR1A as described previously (39).

Field Emission Scanning Electron Microscopy Analysis—To compare the differences in cell surface structure between the WT and mutants, fungal conidia were incubated in SDB at 25 °C for 7 days. The harvested mycelia were washed and fixed overnight in 0.1 M phosphate buffer (pH 7.2) containing a final concentration of 2.5% glutaraldehyde. The samples were dehydrated with a series of ethanol solutions (50–100%, v/v) and coated with platinum. Observations were conducted using a field emission scanning electron microscope (Zeiss) operating at 3 kV (40).

RNA Isolation and Quantitative Real-time PCR (qRT-PCR) Analysis—The mycelia from the WT, Δ*MBZ1*, and Comp that were harvested from 2-day old SDB cultures and from protease induction medium were used for RNA extraction. The samples were homogenized in liquid nitrogen, and total RNA was isolated using TRIzol reagent (Invitrogen) and treated with DNase I (Takara) in a column. cDNA of each sample was generated using an AffinityScript multiple-temperature cDNA synthesis kit (Toyobo). Using the primers for different target genes (Table 1), qRT-PCR analyses were performed using a SYBR Premix Ex *Taq* kit (Takara) with an ABI Prism 7000 sequence detection system (Applied Biosystems). The relative expression of each gene was normalized with reference to the expression of the β-tubulin gene (32).

Yeast One-hybrid Tests—For yeast one-hybrid tests, the cDNA sequence of *MBZ1* was amplified from a cDNA library with primers 1736HF and 1736HR (Table 1) and cloned into the

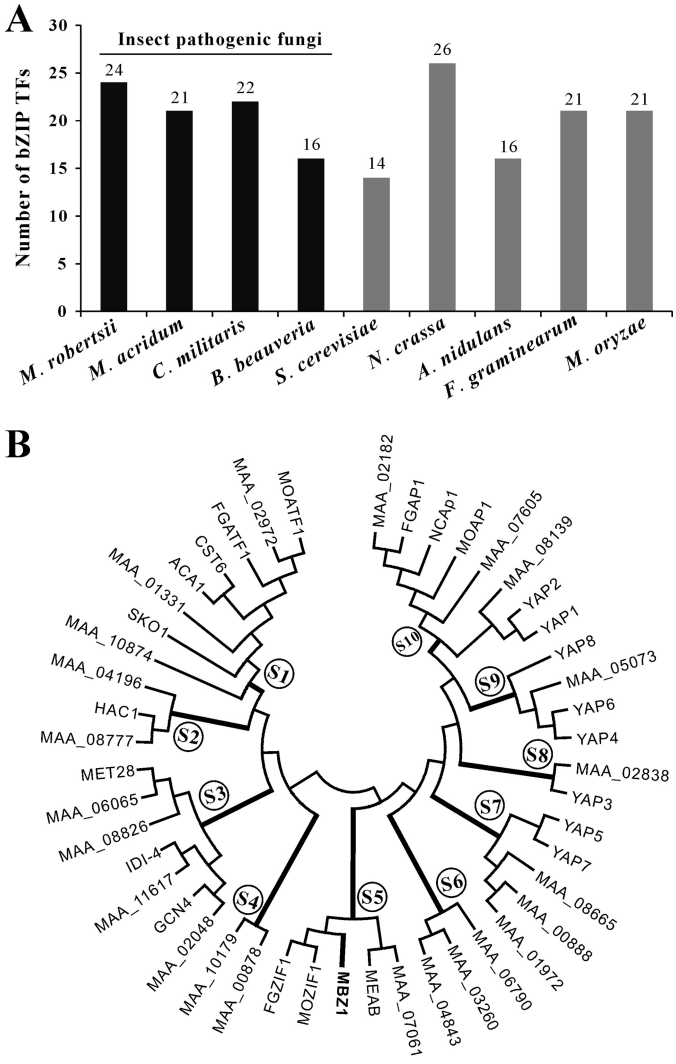

FIGURE 1. **Genome-wide distribution and phylogeny analysis of bZIP-type TFs.** *A*, distribution of bZIP-type TFs in the genomes of selected fungal species. *black* bars indicate insect pathogenic fungi, whereas *gray bars* indicate non-insect pathogenic fungi. *B*, phylogenetic analysis of bZIP-type TFs from *M. robertsii* and *S. cerevisiae* and those that have been functionally studied in different fungi.

SpeI and SacI sites of vector pPC86 under the control of the *GAL4* promoter to generate plasmid pPC86-MBZ1. To test the ability of MBZ1 to bind to the promoter regions of selected genes, promoter fragments were individually amplified by PCR with different primer pairs (Table 1) and inserted into the XhoI site of the p178 vector to control the *lacZ* reporter gene (29). The resultant plasmids were named p178-Xpromoter (where X represents each selected gene). pPC86-MBZ1 and each individual p178-Xpromoter were transformed into yeast strain EGY48 using a small-scale yeast transformation protocol (24). To examine the effect of autoactivation, the yeast cells were transformed only with each p178-Xpromoter vector. Positive colonies were selected on appropriate selection plates (Ura/Trp-free synthetic dropout medium with X-gal). A negative control was generated by transforming the yeast cells with vector pPC86-MBZ1 and a blank vector (p178). A positive control was generated by transforming the yeast cells with vector pPC86-OSBZIP58 and p178-HA2, as used in a previous study (29). The

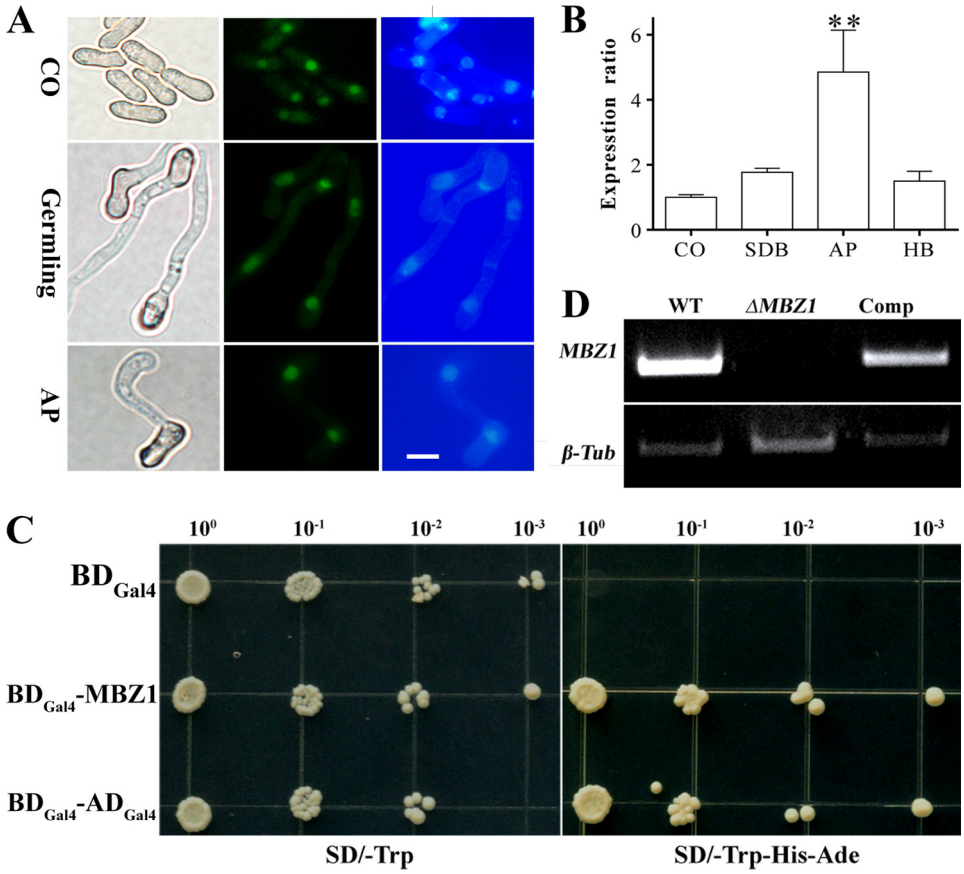

FIGURE 2. **Characterization of MBZ1 and verification of gene deletion.** *A*, localization assay of the MBZ1 protein in *M. robertsii*. GFP-MBZ1 is localized in the nuclei of conidia (*CO*), germlings (spores germinated in SDB for 18 h), and appressoria (*AP*; formed on hydrophobic surface 18 h post-inoculation) as shown by co-localization with florescent Hoechst staining. *Scale bar* = 5 μm. *B*, qRT-PCR analyses of *MBZ1* expression by the fungus at the stages of conidiation, saprophytic growth in SDB, appressorium formation, and hyphal body (*HB*) formation in insect hemolymph. **, $p < 0.01$. *C*, transcriptional activation tests in yeast. Yeast strain AH109 carrying fusion cassettes of the GAL4 DNA-binding domain (DB_{Gal4}; negative control), the GAL4 DNA-binding and activation domains (DB_{Gal4}-AD_{Gal4}; positive control), or *MBZ1* were cultured on synthetic dropout (*SD*) medium at 30 °C for 3 days. *D*, verification of *MBZ1* gene deletion by RT-PCR. The fungi were grown in SDB for 48 h and used for RNA extraction for analysis. A β-tubulin gene (β-*Tub*) was used as a reference.

blue colonies obtained indicated positive interactions, whereas the white colonies indicated no binding.

RESULTS

Characteristics of MBZ1—Genome-wide analysis indicated that there are 24 bZIP domain-containing TFs encoded in the genome of *M. robertsii*, whereas 14–26 bZIP-type TFs are present in yeast and other fungi (Fig. 1*A*). Overall, the number of bZIP TFs present in fungi are >2-fold fewer than those found in humans (56 bZIP genes) and plants (*e.g.* 75 in *Arabidopsis*, 89 in rice, and 125 in maize) (4). A phylogenetic analysis based on the bZIP domain sequences indicated that *M. robertsii* bZIP-type TFs could be classified into at least 10 subfamilies (Fig. 1*B*). Subfamilies 4–6 have no homologs in yeast. The MBZ1 protein belongs to subfamily 5 and shares higher homology with its counterparts FGZIF1 (FGSG_01555, 57% identity) of *F. graminearum* and MOZIF1 (MGG_03288, 45% identity) of *M. oryzae* (10), but is only moderately homologous to MeaB (AN4900, 11% identity) of *A. nidulans* (7). All these TFs belong to subfamily 5 (Fig. 1*B*). In particular, subfamily 1 contains the yeast proteins CST6, ACA1, and SKO1 (Fig. 1*B*), which belong to the cAMP response element-binding protein (CREB) family of bZIP-type TFs that bind the consensus palindromic site 5′-TGACGTCA-3′ (41).

To verify the nuclear localization of MBZ1, a *GFP* gene was fused with the 5′ terminus of *MBZ1* for transformation of *M. robertsii*. Fluorescence microscopy examinations verified that the GFP signal could be detected only in the nuclei of fungal spores, germlings, and appressoria of *M. robertsii* (Fig. 2*A*). Consistent with our previous RNA-seq analysis (16), a qRT-PCR analysis confirmed that *MBZ1* was most highly transcribed by the fungus during infection structure appressorium formation compared with the stages of fungal conidiation, saprophytic growth, and differentiation of hyphal bodies (blastospores formed in the insect body cavity) (Fig. 2*B*). A transcriptional activation test indicated that, relative to a negative control, yeast cells transformed with a vector containing *MBZ1* cDNA could survive on an auxotrophic medium, as could the positive control yeast cells engineered with a GAL4 activation domain (Fig. 2*C*). The results thereby confirmed the typical TF characteristics of MBZ1: nuclear localization and transcriptional activation.

Gene Deletion and Phenotype Characterization—To study gene function, *MBZ1* was disrupted via homologous replacement. The null mutant was complemented with the full *MBZ1* ORF and designated Comp, which was verified by PCR and RT-PCR analyses. In contrast to the WT and Comp strains,

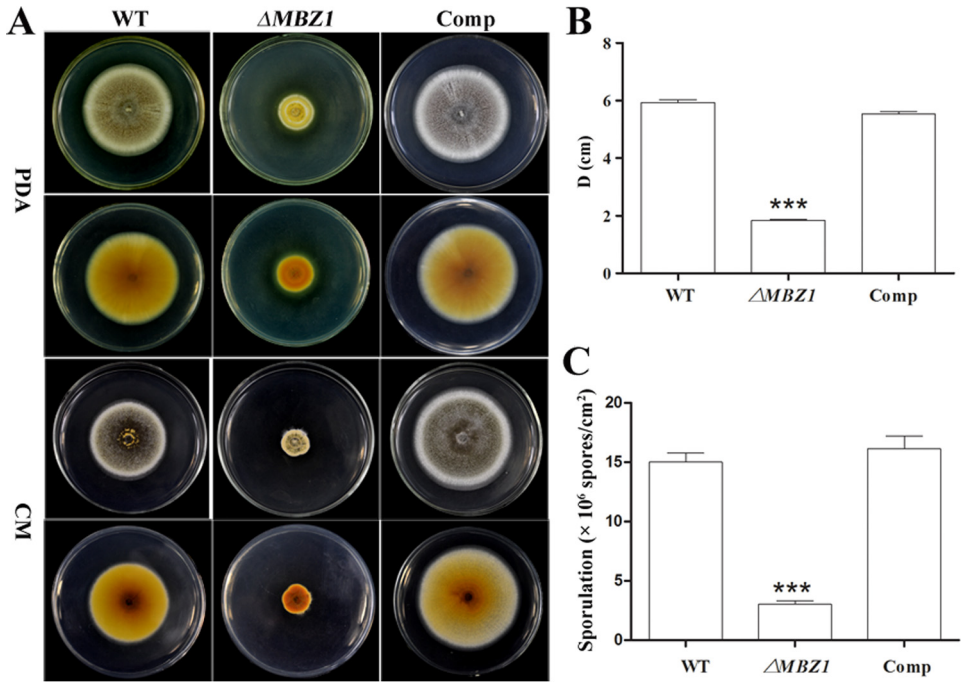

FIGURE 3. **MBZ1 is required for normal growth and sporulation in *M. robertsii*.** *A*, phenotypic variation. Cultures of the WT, Δ*MBZ1*, and Comp were grown on PDA and complete mineral medium (*CM*) for 14 days. *B*, colony diameter (*D*) variations among different cultures. *Error bars* represent S.E. from three replicates. *C*, variation in spore production by the WT, Δ*MBZ1*, and Comp after growing the fungi on PDA for 2 weeks. ***, $p < 0.001$.

MBZ1 gene transcription was eliminated in Δ*MBZ1* (Fig. 2*D*). Growth assays revealed that Δ*MBZ1* showed impaired growth and sporulation on PDA and complete mineral medium after 2 weeks of growth (Fig. 3*A*). Relative to the WT (5.93 ± 0.75 cm) and Comp (5.53 ± 1.04 cm), the colony diameter of Δ*MBZ1* (1.83 ± 0.27 cm) was reduced significantly ($p < 0.001$) after incubation on PDA (Fig. 3*B*). In addition, the sporulation of Δ*MBZ1* ((3.03 ± 0.04) × 10^6 conidia/cm^2) was also significantly impaired ($p < 0.001$) compared with the WT ((14.99 ± 0.09) × 10^6 conidia/cm^2) and Comp ((16.14 ± 0.09) × 10^6 conidia/cm^2) (Fig. 3*C*). Deletion of *MBZ1* also altered culture pigmentation, *i.e.* Δ*MBZ1* (but not the WT and Comp) accumulated yellow pigments in its mycelia when grown on PDA (Fig. 4*A*).

Deletion of MBZ1 Impairs Cell Wall integrity—We performed experiments to test the sensitivities of the WT, Δ*MBZ1*, and Comp in response to different cell wall stressors or biosynthesis inhibitors. The observations indicated that the *MBZ1* null mutant (but not the WT and Comp) lost the ability to grow on PDA supplemented with Congo red (Fig. 5*A*). However, no significant differences were found between the WT and mutants regarding growth in the presence of tunicamycin, Calcofluor White, amphotericin B, $CuSO_4$, sorbitol, DTT, or SDS (data not shown). Congo red also inhibited mutant spore germination in SDB. Relative to the WT (68.89 ± 7.83%) and Comp (58.40 ± 8.90%), the germination rates of Δ*MBZ1* spores (11.95 ± 2.80%) were significantly reduced ($p < 0.001$) after incubation for 24 h (Fig. 5*B*).

As indicated above, Δ*MBZ1* became sensitive to Congo red, but not Calcofluor White. We speculated that the cell wall components, especially the chitin content, would be altered in the *MBZ1* null mutant. To test this, we performed a chitin quantification assay, which revealed that the level of chitin in the

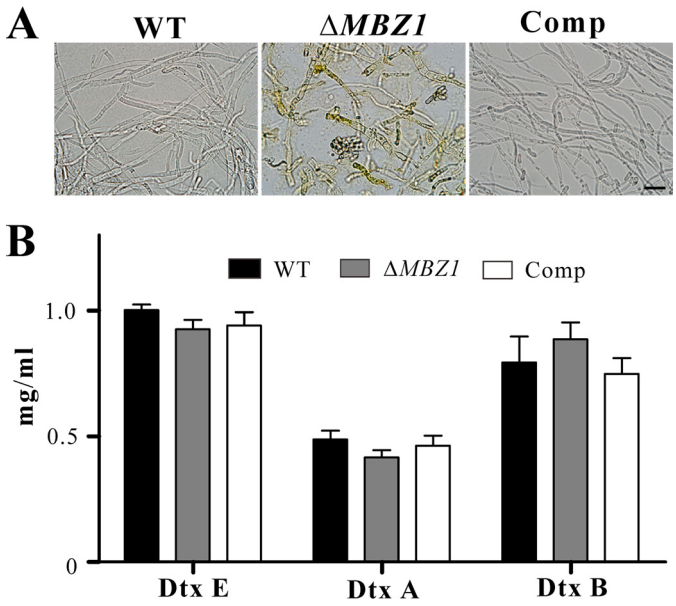

FIGURE 4. *A*, mycelia of the WT, Δ*MBZ1*, and Comp on PDA after 2 weeks of growth. *Scale bar* = 20 μm. *B*, quantification and comparison of cyclopeptide destruxins (*Dtx*) produced by the WT and mutants. The results indicate no significant differences between the WT and mutants, suggesting that MBZ1 is not involved in controlling destruxin production.

Δ*MBZ1* cell wall (8.62 ± 0.82%) was significantly increased ($p < 0.05$) compared with the WT (4.19 ± 0.95%) and Comp (3.74 ± 0.11%) (Fig. 5*C*). In addition, we performed cell wall binding assays with concanavalin A, *G. simplicifolia* lectin II, and *G. nivalis* lectin (24, 25). The results demonstrated a stronger fluorescent signal for Δ*MBZ1* cells when stained with *G. simplicifolia* lectin II, suggesting again a higher level of chitin accumulation compared with the WT and Comp. No apparent

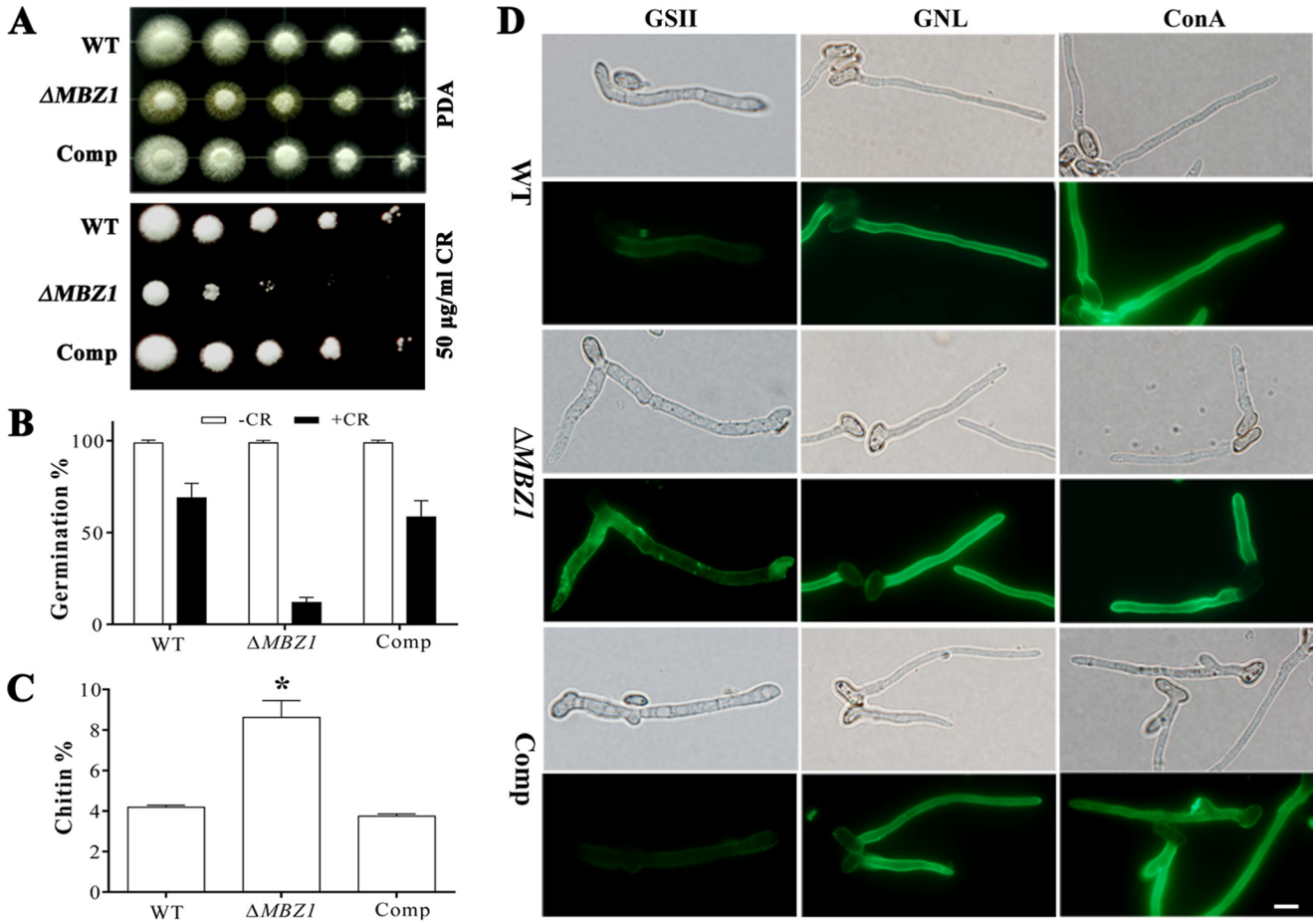

FIGURE 5. **Impairment of cell wall integrity.** *A*, effect of the cell wall inhibitor Congo red (*CR*) on fungal growth. Two microliters of 10-fold serial dilutions of spore suspensions (5×10^7 conidia/ml) were inoculated on PDA plates with or without Congo red and incubated at 28 °C for 72 h. *B*, germination rates of the WT and mutants in SDB with or without Congo red (50 μg/ml) 24 h post-inoculation. *Error bars* represent S.E. from three replicates. *C*, chitin quantification. Each *bar* represents the mean ± S.E. from two independent experiments, and each treatment had three replicates. *, $p < 0.05$. *D*, fluorescence lectin staining. Conidia of the WT and mutants were germinated in SDB for 12 h before staining with *G. simplicifolia* lectin II (*GSII*), *G. nivalis* lectin (*GNL*), and concanavalin A (*ConA*). *Scale bar* = 5 μm.

differences were found between the WT and mutants for the treatments with concanavalin A and *G. nivalis* lectin (Fig. 5*D*).

Impairment of Conidial Hydrophobicity and Adherence to Hydrophobic Surface—Consistent with the impairment of cell wall integrity, the hydrophobicity defect in the Δ*MBZ1* spores was also found during the preparation of spore suspensions. Thus, unlike the WT and Comp, Δ*MBZ1* conidia were more readily dispersible in water without the detergent Tween 20 (Fig. 6*A*). Ultrastructure examinations of spore surface features did not reveal any morphological difference between the WT and mutants (Fig. 6*B*). However, the measurements of cell surface hydrophobicity indicated that the hydrophobicity index of Δ*MBZ1* spores (0.39 ± 0.09) was significantly reduced ($p <$ 0.01) compared with the WT (0.88 ± 0.02) and Comp (0.81 ± 0.05) (Fig. 6*C*). In addition, a quantitative assay of cell adhesion ability demonstrated that Δ*MBZ1* had a significantly impaired capacity ($p < 0.001$) to bind to a hydrophobic surface compared with the WT and Comp (Fig. 6*D*).

Deletion of MBZ1 Impairs Fungal Virulence—To examine the effect of *MBZ1* deletion on fungal virulence, we performed both topical infection and injection bioassays with last-instar silkworm and wax moth larvae. The LT_{50} values were estimated and compared among the WT, Δ*MBZ1*, and Comp. After topical infection of silkworms, the differences were significant between the WT ($LT_{50} = 2.8 \pm 0.09$ days) and Δ*MBZ1* ($LT_{50} = 3.9 \pm 0.13$ days) ($\chi^2 = 25.12$, $p < 0.0001$) and between Δ*MBZ1* and Comp ($LT_{50} = 2.8 \pm 0.08$ days) ($\chi^2 = 29.33$, $p < 0.0001$) (Fig. 7*A*). However, there was no significant difference in injection assays among the WT ($LT_{50} = 2.8 \pm 0.10$ days), Δ*MBZ1* ($LT_{50} = 2.7 \pm 0.10$ days), and Comp ($LT_{50} = 2.7 \pm 0.10$ days) ($p > 0.5$) (Fig. 7*B*). Similar patterns were observed during the topical infection and injection assays using the wax moth larvae (Fig. 7, *C* and *D*). Thus, MBZ1 is required for the virulence of *M. robertsii* by playing a role in fungal adhesion to and penetration of the insect cuticle. The results are consistent with the qRT-PCR data that the expression of *MBZ1* was highly activated by the fungus during early infection, but not during growth in insect blood (Fig. 2*B*). In support of this, the melanization spots characteristic of fungal penetration were not evident on the insects topically treated with the Δ*MBZ1* spores, but were abundant on the insects treated with the WT and Comp conidia 48 h post-inoculation (Fig. 7*E*).

Negative Regulation of Protease Activity—The impact of *MBZ1* deletion on spore adhesion and hydrophobicity contributes to virulence defects in Δ*MBZ1*. To examine whether any other virulence factors were affected, we performed infection

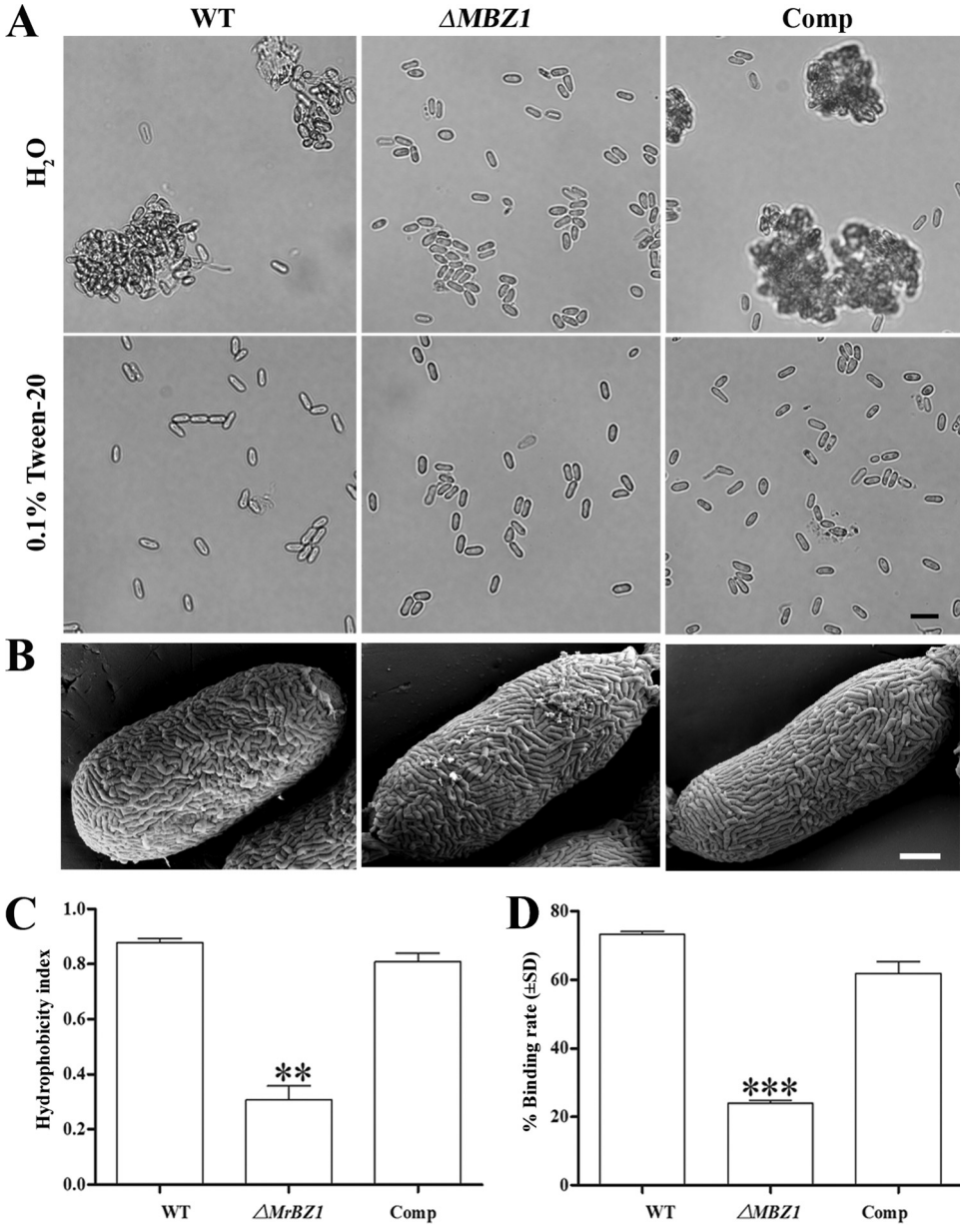

FIGURE 6. **Analyses of spore hydrophobicity and adherence ability.** *A*, variation in spore dispersal ability between the WT and mutants in water and 0.1% Tween 20. *Scale bar* = 10 μm. *B*, spore surface structures examined by field emission scanning electron microscopy analysis. *Scale bar* = 1 μm. *C*, variation in spore surface hydrophobicity between the WT and mutants. **, $p < 0.01$, WT (or Comp) *versus* Δ*MBZ1*. *D*, variation in spore ability to adhere to hydrophobic surfaces between the WT and mutants. ***, $p < 0.001$, WT (or Comp) *versus* Δ*MBZ1*.

structure induction. The results indicated that the spores of Δ*MBZ1* could similarly form appressoria like the WT and Comp on both hydrophobic surfaces and insect cuticles (Fig. 8). In addition, we found that the biosynthesis of insecticidal cyclopeptide destruxins was not affected in Δ*MBZ1* compared with the WT and Comp (Fig. 4*B*). We also tested the expression of cuticular degradation proteases. After growth in SDB for 48 h, unexpectedly, the subtilisin-like protease activity of Δ*MBZ1* was significantly increased ($p < 0.001$) compared with the WT and Comp. However, the differences were not significant among the isolates when they were grown in the inductive medium containing insect homogenates (Fig. 9*A*). These observations were confirmed by Western blot analysis using an antibody against PR1A, an extracellular protease (Fig. 9*B*). In addition, consistent with a previous analysis (42), the expression of proteases was switched off in both the WT and Δ*MBZ1* when the fungi were grown in insect blood (Fig. 9*B*). These findings suggest that MBZ1 is involved only in the negative control of protease expression during fungal saprophytic growth in artificial and nutrient-rich media, but not in insect component-containing substrates. This was further evidenced when the cell surface mucilage-like structures found in Δ*MBZ1* (but not in the WT and Comp) were self-digested when grown in SDB (Fig. 9*C*). This phenotype is similar to fungal cell autolysis (43).

Verification of Transcriptional Control of Target Genes—As indicated above, the cell wall integrity of Δ*MBZ1* was impaired, and expression of proteases was activated in artificial medium. To verify the control of downstream genes by *MBZ1*, the puta-

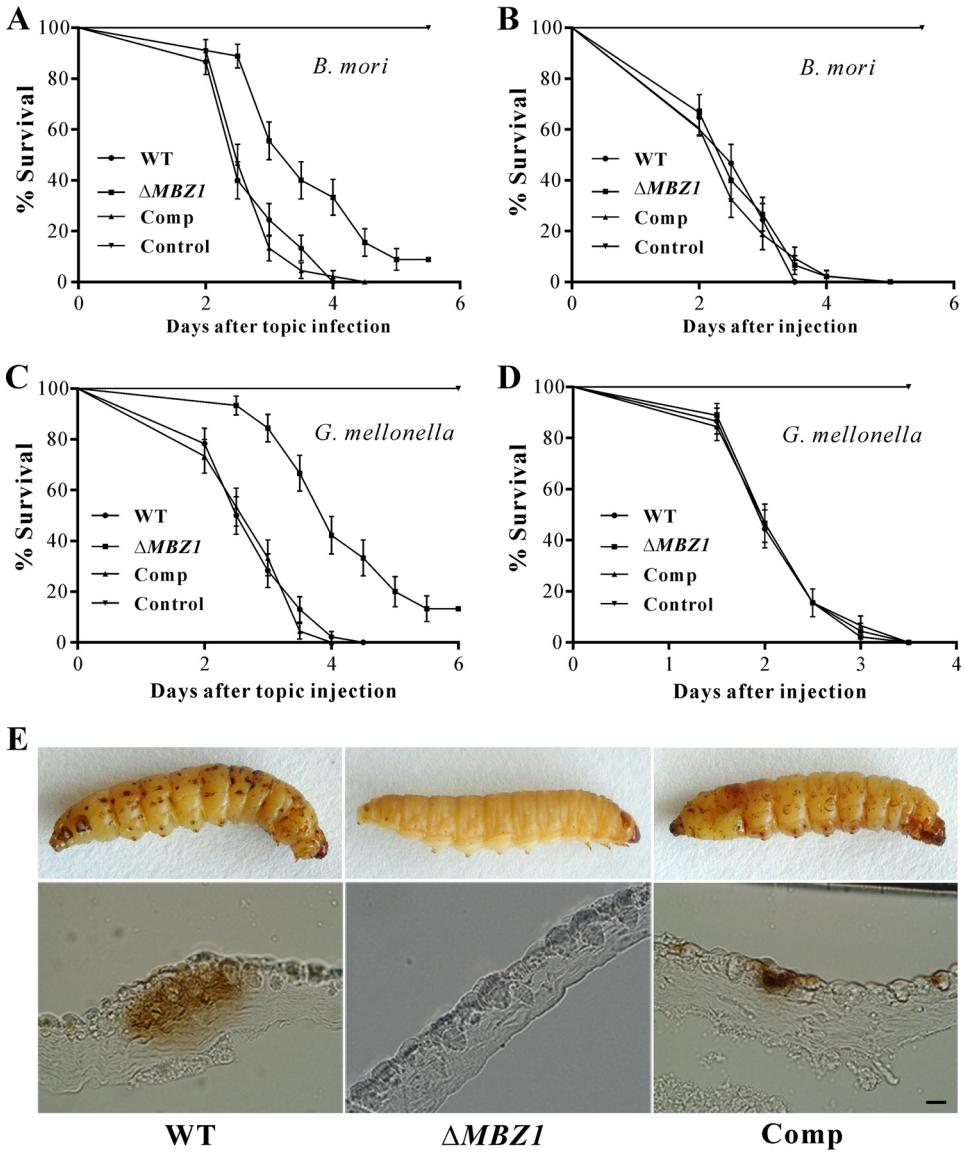

FIGURE 7. **Insect bioassays.** *A*, survival of silkworm larvae following topical infection with the spore suspensions (1×10^7 spores/ml) of the WT and mutants. *B*, survival of silkworm larvae following injection with the spore suspensions (10 μl, 1×10^6 spores/ml) of the WT and mutants. Control insects were treated with sterile water. *C*, survival of wax moth larvae following topical infection with the spore suspensions (1×10^7 spores/ml). *D*, survival of wax moth larvae following injection with the spore suspensions (10 μl, 1×10^6 spores/ml). Control insects were treated with sterile water. *Error bars* represent S.D. *E*, impairment of topical infection in Δ*MBZ1*. The wax moth larvae were topically infected for 48 h and embedded for cutting and microscopic observations. Relative to the WT and Comp, many fewer melanization spots were observed on the insects treated with Δ*MBZ1* spores. *Scale bar* = 1 mm.

tively targeted genes were selected for qRT-PCR analysis and yeast one-hybrid tests for promoter binding. These included the cell wall biosynthesis-related genes, protease genes, and the adhesin gene *MAD1* (Table 2). After growth in SDB for 48 h, the putative β-1,3-glucanosyltransglycosylases (MAA_01794, similar to yeast GAS2, 39% identity; and MAA_02558, similar to yeast GAS3, 39% identity) and cell wall glucanosyltransferases (MAA_02062 and MAA_04636, both similar to the yeast chitin transglycosylase CRH1 with 44 and 31% identities, respectively) were significantly down-regulated in Δ*MBZ1* compared with the WT (Table 3). In contrast, the gene MAA_07202, which is highly similar to the yeast glutamine:fructose-6-phosphate amidotransferase GFA1 (60% identity) involved in chitin biosynthesis (44, 45), was up-regulated by >6-fold in Δ*MBZ1* (Table 3). The adhesin MAD1 (MAA_03775) mediates conidial adherence to hydrophobic surface in *Metarhizium* (46). Relative to the WT, the *MAD1* gene was down-regulated by 4-fold in Δ*MBZ1*. This was therefore consistent with the defect of spore adherence ability in Δ*MBZ1* (Fig. 6*C*). Consistent with the increase in protease activity in SDB (Fig. 9, *A* and *B*), the subtilisin-like protease genes, *e.g.* the *PR1A* gene (MAA_05675), were significantly up-regulated in Δ*MBZ1* compared with the WT (Table 3).

In silico analysis identified the presence of the conserved motif 5′-TGACG-3′ in the promoter regions of all selected genes (Fig. 10*A*), which is the functional half-site of the CREB-targeting palindrome (5′-TGACGTCA-3′) (47), suggesting that MBZ1 is also the CREB site or half-site activator. Heterologous expression of *MBZ1* in *Escherichia coli* failed to obtain soluble protein for the electrophoretic mobility shift assay. To verify the binding of MBZ1 to the promoter regions of these

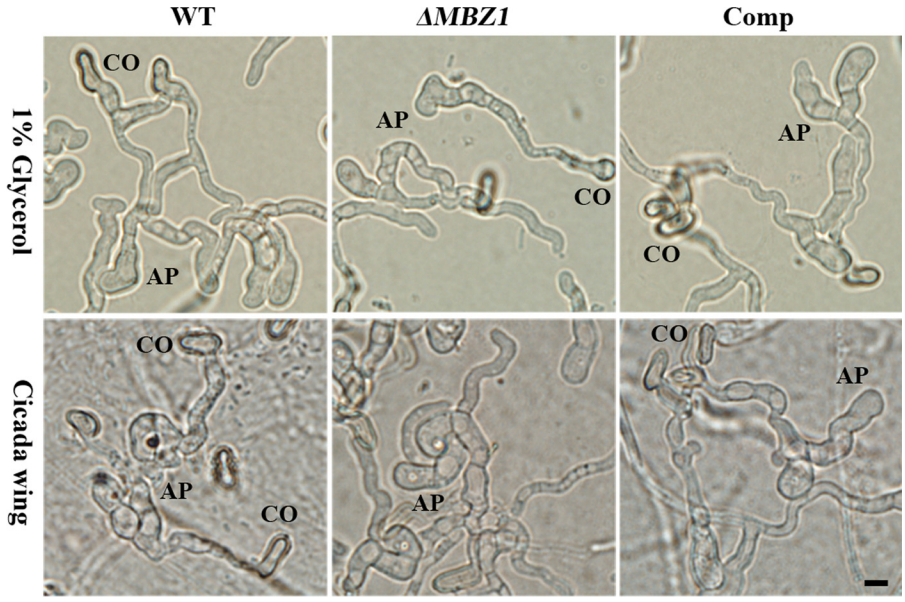

FIGURE 8. **Appressorium induction.** The conidia (*CO*) of the WT, Δ*MBZ1*, and Comp were inoculated on hydrophobic surfaces (*upper panels*) or cicada hind wings (*lower panels*) and incubated for 24 h for appressorium (*AP*) induction. *Scale bar* = 5 μm.

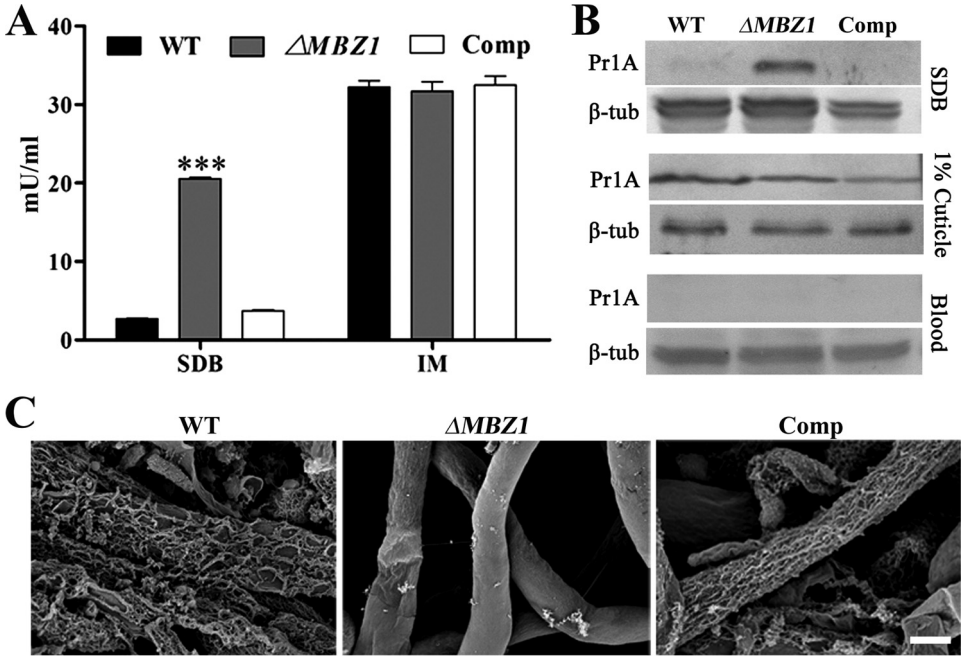

FIGURE 9. **Up-regulation of proteases in Δ*MBZ1*.** *A*, protease activity assay. The spores of the WT, Δ*MBZ1*, and Comp were cultured in SDB and inductive medium (*IM*; 1% cuticle) for 48 h, and the supernatants were harvested for protease activity assay. ***, $p < 0.001$. *B*, Western blot analysis. The supernatant samples from *A* and insect blood (hemolymph) collected 48 h after injection with fungal spores were used for analysis with the anti-PR1A protease polyclonal antibody. *C*, Examination of cell surface structure. The spores of the WT, Δ*MBZ1*, and Comp were cultured in SDB for 7 days, and the mycelia were harvested, washed twice with distilled water, and used for field emission scanning electron microscopy microscope analysis. *Scale bar* = 1 μm.

target genes, we performed yeast one-hybrid assays. The yeast cells transformed with only the individual promoter region could not express β-galactosidase, *i.e.* the preclusion of self-activation (Fig. 10*B*). Except for the promoters of *MAD1* and the *GFA1*-like gene (MAA_07202), the β-galactosidase activity was activated by MBZ1 when under the control of the selected gene promoters (Fig. 10*C*). However, consistent with a previous report (28), the reporter enzyme activity varied among the controls with different gene promoters. The highest binding and activation activities were observed for MBZ1 toward the *GAS2* (MAA_01794) and *GAS3*-like (MAA_02558) genes (Fig. 10*C*). Interestingly, the full CREB site is present in the promoter of MAA_01794, but it is the 5′-TGACGTTG-3′ for MAA_02558 (Fig. 10*A*).

DISCUSSION

In this study, we characterized the functions of the bZIP-type TF MBZ1 in the insect pathogenic fungus *M. robertsii*. Gene deletion, biochemical analyses, and insect bioassays indicated that MBZ1 contributes to the regulation of fungal growth,

TABLE 2

Information of selected putative target genes for qRT-PCR and yeast one-hybrid analyses

NA, not available.

Gene	Description	Yeast homolog (% identity)	Primers for qRT-PCR/yeast one-hybrid analyses
MAA_01794	β-1,3-Glucanosyltransglycosylases	GAS2 (39%), GAS1 (36%)	1794F, 1794R/1794YF, 1794YR
MAA_02558	β-1,3-Glucanosyltransglycosylases	GAS3 (39%), GAS4 (38%), GAS5 (35%)	2558F, 2558R/2558YF, 2558YR
MAA_04636	Cell wall glucanosyltransferase	CRH1 (44%)	4636F, 4636R/4636YF, 4636YR
MAA_02062	Cell wall glucanosyltransferase	CRH1 (31%)	2062F, 2062R/2062YF, 2062YR
MAA_07202	Glutamine:fructose-6-phosphate amidotransferase	GFA1 (60%)	7202F, 7202R/7202YF, 7202YR
MAA_02408	Subtilisin-like serine protease PR1J	NA	2408F,2408R/2408YF, 2408YR
MAA_05675	Subtilisin-like serine protease PR1A	NA	5675F, 5675R/5675YF, 5675YR
MAA_10246	Subtilisin-like protease	NA	10246F, 10246R/10246YF, 10246YR
MAA_10260	Subtilisin-like protease PR1H	NA	10260F, 10260R/10260YF, 10260YR
MAA_03775	Adhesin protein MAD1	NA	3775F, 3775R/3775YF, 3775YR

TABLE 3

Differential expression of selected genes by the WT and mutants of *M. robertsii*

The fungi were grown in SDB, or newly harvested conidia were used for RNA extraction and subsequent qRT-PCR analysis. A β-tubulin gene was used as a reference.

Gene	WT	Δ*MBZ1*	Comp
Cell wall-associated genes			
MAA_02558	1.00 ± 0.13	0.079 ± 0.048[a]	1.36 ± 0.51
MAA_01794	0.013 ± 0.0013	0.0021 ± 0.00016[a]	0.020 ± 0.0023
MAA_07404	0.22 ± 0.057	0.019 ± 0.00060[a]	0.29 ± 0.013
MAA_04636	10.08 ± 0.75	0.82 ± 0.042[a]	16.20 ± 3.97
MAA_07202	0.70 ± 0.12	4.73 ± 0.81[a]	0.92 ± 0.27
Adhesin *MAD1*			
MAA_03775	1.00 ± 0.21	0.25 ± 0.095[a]	1.78 ± 0.94
Subtilisin protease genes			
MAA_02048	1.00 ± 0.18	6.58 ± 0.65[b]	2.97 ± 0.62
MAA_05675	2.44 ± 0.25	26.13 ± 2.36[b]	6.23 ± 1.02
MAA_10246	0	0.33 ± 0.04[b]	0
MAA_10260	0	11.88 ± 1.36[b]	0

[a] $p < 0.05$ between Δ*MBZ1* and WT or between Δ*MBZ1* and Comp.
[b] $p < 0.01$ between Δ*MBZ1* and WT or between Δ*MBZ1* and Comp.

conidiation, cell wall integrity, and virulence. Enzyme activity, Western blotting, and qRT-PCR analyses demonstrated that MBZ1 is involved in both the positive and negative transcriptional control of various target genes, which is similar to the regulation pattern of the C2H2-type pH-responsive regulator of *M. robertsii* (32). Similar to virulence defects in gene deletion mutants of *FGZIF1* in *F. graminearum* and *MOZIF1* in *M. oryzae* (10), Δ*MBZ1* was impaired in killing insects. Interestingly, Δ*FGZIF1* does not show defects in maintenance of cell wall integrity (*i.e.* not sensitive to Congo red), conidiation, and growth (10). This is in contrast to our observations for Δ*MBZ1*, which suggests that, in addition to the functional divergence of paralogous bZIP-type TFs (15), the orthologous TFs could play divergent roles in different organisms. Deletion of the bZIP-type TF gene *FGAP1* does not affect the pathogenicity of *F. graminearum* to wheat (11), but loss of the orthologous gene *MOAP1* in *M. oryzae* completely abolishes its pathogenicity to rice (14). Likewise, other studies have found that the null mutants of *MOATF1* of *M. oryzae* and *FGATF1* of *F. graminearum* have reduced virulence, but the former are more sensitive to oxidative stress (12, 13). We also observed that deletion of *MBZ1* affected fungal pigmentation (Figs. 3*A* and 4*A*), but not production of insecticidal mycotoxin destruxins (Fig. 4*B*). In *F. graminearum*, however, deletion of *FGZIF1* significantly impairs fungal production of the mycotoxin deoxynivalenol (a type B trichothecene) (10). Thus, the functional divergence of these orthologs in the different fungal species would question the assumption of ortholog conjecture, which suggests that orthologous genes carry out equivalent biological functions in different organisms (48). However, it remains to be determined whether the orthologs from plant pathogens could fully complement the phenotypes of Δ*MBZ1* in *M. robertsii*.

The teleomorph of *Metarhizium* spp. is considered to be *Metacordyceps* spp.; however, their heterothallic sexual cycles are largely cryptic (49). Future studies are still required to investigate whether MBZ1 is involved in controlling sexuality in *M. robertsii* as FGZIF1 and FGATF1 control sex cycles in *F. graminearum* (10, 12). The fungal cell wall plays essential roles in mediating growth, stress resistance, cell adhesion to hosts, and infection (50). We found that deletion of *MBZ1* led to the down-regulation of *GH72*-like genes (MAA_01794 and MAA_02558) and yeast *CRH1*-like genes (MAA_02062 and MAA_04636), but led to the up-regulation of the *GFA1*-like gene MAA_07202. The GH72 family of glycosidases/transglycosidases plays important roles in cell wall maintenance (51). Deletion mutants of these genes have defects in cell adherence to hydrophobic surfaces and increases in chitin in the cell wall (52, 53). The yeast chitin transglycosylase CRH1 acts to transfer chitin and cross-link it to β-1,3- and β-1,6-glucans in the cell wall (54), and GFA1 contributes to the first step of chitin biosynthesis (44). Relative to the WT, differential regulation of these genes would be responsible for chitin accumulation in the Δ*MBZ1* cell wall and therefore the increased sensitivity to the chitin-specific dye Congo red (Fig. 5*A*). However, the Congo red sensitivity was not observed for Δ*FGZIF1* (10), but it was observed for Δ*FGATF1* of *F. graminearum* (12). This is again suggestive of the functional divergence of orthologous bZIP TFs among different species. In *Candida albicans*, deletion of the *GH72*-like *PHR2* gene (homologous to yeast *GAS2* and *GAS3*) additionally results in sporulation failure (52, 53). Thus, the down-regulation of *GH72*-like genes could contribute, at least in part, to the defective conidiogenesis in Δ*MBZ1* (Fig. 3). However, it remains to be determined how *MBZ1* is involved in mediating mycelial growth in *M. robertsii*; the effect has not been observed for its counterpart *FGZIF1* in *F. graminearum* (10).

We tested virulence via both topical infection and injection assays against two different insect species and found that differences were observed only between the WT and Δ*MBZ1* with topical infections (Fig. 7), suggesting that the null mutant can evade host immunity within the insect hemocoel as well as the WT. Because Δ*MBZ1* could successfully produce the infection

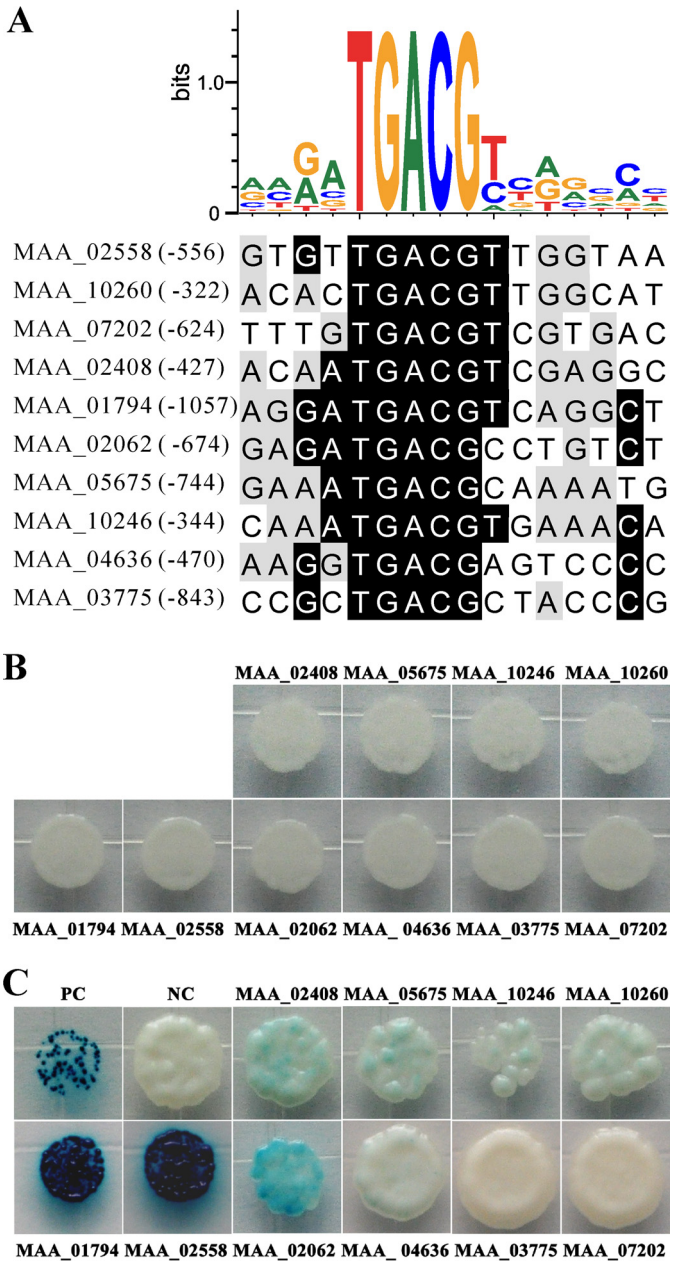

FIGURE 10. **Analysis of putative MBZ1-binding site and yeast one-hybrid tests.** *A*, identification of the consensus binding site present in the promoter regions of target genes. *B*, autoactivation tests. Yeast cells transformed with only the p178 vector containing each individual promoter did not show autoactivation activities. *C*, verification of transcription control of target genes by MBZ1 in yeast. Yeast cells were transformed with both the p178 vector containing each individual promoter and plasmid pPC86-MBZ1 containing *MBZ1* cDNA. *PC*, positive control; *NC*, negative control.

structure appressorium (Fig. 8), failure to bind to the insect cuticle would be mainly responsible for the defective virulence in Δ*MBZ1* due to the reduction of its surface hydrophobicity and adherence ability. This resembles the effect of deletion of the adhesin *MAD1* gene in *M. robertsii* (46). The subtilisin proteases are the key virulence factors of insect pathogenic fungi for degradation of insect cuticular proteins (42). Overexpression of the protease PR1A increases fungal virulence and causes extensive melanization of infected insects due to the activation of insect prophenoloxidases (39, 55). Interestingly, the up-regulation of proteases in Δ*MBZ1* was observed only when the fungus was grown in artificial medium, but not in insect component-related conditions. This was particularly clear when proteases were successfully switched off in insect hemolymph (Fig. 9*B*). The result suggests that there are additional TFs involved in fine-tuning protease expression in *M. robertsii*. In filamentous fungi, the Zn_2Cys_6 domain-containing TF PrtT has been characterized as an activator of extracellular proteases (56). A homolog of *Aspergillus* PrtT is also present in the genome of *M. robertsii* (MAA_09737, 24% identity) (16). Thus, the mechanisms used by MBZ1 to regulate protease expression, as well as the possible interactions between MBZ1 and other TFs, remain to be clarified.

The formation of either homodimers or heterodimers is the hallmark of bZIP-type TFs, which allows them to increase the complexity of regulatory networks (2). Our results indicate that deletion of *MBZ1* resulted in up-regulation of a *GFA1*-like gene (MAA_07202) and down-regulation of the adhesin gene in *M. robertsii* (Table 3). Cell adhesion assays also revealed the significantly reduced ability of Δ*MBZ1* spores to bind to hydrophobic surfaces (Fig. 6*D*). The CREB half-site is present in the promoter regions (Fig. 10*A*); however, yeast one-hybrid assays showed that MBZ1 did not bind to the promoter regions of *MAD1* and the *GFA1*-like gene (Fig. 10*C*). Precluding the possibility of a technical false-negative or false-positive issue, the findings suggest the possible formation of heterodimerized MBZ1 in the regulation of these genes, *i.e.* the indirect control of these target genes. The putative partner involved in dimerization with MBZ1 remains to be determined.

In conclusion, we characterized the bZIP-type TF MBZ1 in an insect pathogenic fungal model and established that the *MBZ1* gene is required for virulence against insects by mediating cell wall integrity, cell surface hydrophobicity, and adherence to hydrophobic surfaces. Both negative and positive regulation of various target genes was evident, indicating that MBZ1 can function as either an activator or a suppressor. The results of this study also reveal the functional divergence of orthologous bZIP-type TFs in different fungal species, highlighting the need to elucidate orthologous gene function in different organisms.

Acknowledgments—We thank Brian R. Lovett (University of Maryland) for critical reading of this manuscript and Xiaoyan Gao for help with the imaging analyses.

REFERENCES

1. Wagner, E. F. (2001) AP-1–introductory remarks. *Oncogene* **20,** 2334–2335
2. Amoutzias, G. D., Veron, A. S., Weiner, J., 3rd, Robinson-Rechavi, M., Bornberg-Bauer, E., Oliver, S. G., and Robertson, D. L. (2007) One billion years of bZIP transcription factor evolution: conservation and change in dimerization and DNA-binding site specificity. *Mol. Biol. Evol.* **24,** 827–835
3. Landschulz, W. H., Johnson, P. F., and McKnight, S. L. (1988) The leucine zipper: a hypothetical structure common to a new class of DNA binding proteins. *Science* **240,** 1759–1764
4. Llorca, C. M., Potschin, M., and Zentgraf, U. (2014) bZIPs and WRKYs: two large transcription factor families executing two different functional strategies. *Front. Plant Sci.* **5,** 169

5. Moye-Rowley, W. S., Harshman, K. D., and Parker, C. S. (1989) Yeast *YAP1* encodes a novel form of the Jun family of transcriptional activator proteins. *Genes Dev.* **3,** 283–292
6. Fernandes, L., Rodrigues-Pousada, C., and Struhl, K. (1997) Yap, a novel family of eight bZIP proteins in *Saccharomyces cerevisiae* with distinct biological functions. *Mol. Cell. Biol.* **17,** 6982–6993
7. Polley, S. D., and Caddick, M. X. (1996) Molecular characterisation of *meaB*, a novel gene affecting nitrogen metabolite repression in *Aspergillus nidulans*. *FEBS Lett.* **388,** 200–205
8. Yin, W. B., Reinke, A. W., Szilágyi, M., Emri, T., Chiang, Y. M., Keating, A. E., Pócsi, I., Wang, C. C., and Keller, N. P. (2013) bZIP transcription factors affecting secondary metabolism, sexual development and stress responses in *Aspergillus nidulans*. *Microbiology* **159,** 77–88
9. Tian, C., Li, J., and Glass, N. L. (2011) Exploring the bZIP transcription factor regulatory network in *Neurospora crassa*. *Microbiology* **157,** 747–759
10. Wang, Y., Liu, W., Hou, Z., Wang, C., Zhou, X., Jonkers, W., Ding, S., Kistler, H. C., and Xu, J. R. (2011) A novel transcriptional factor important for pathogenesis and ascosporogenesis in *Fusarium graminearum*. *Mol. Plant Microbe Interact.* **24,** 118–128
11. Montibus, M., Ducos, C., Bonnin-Verdal, M. N., Bormann, J., Ponts, N., Richard-Forget, F., and Barreau, C. (2013) The bZIP transcription factor Fgap1 mediates oxidative stress response and trichothecene biosynthesis but not virulence in *Fusarium graminearum*. *PLoS ONE* **8,** e83377
12. Jiang, C., Zhang, S., Zhang, Q., Tao, Y., and Xu, J. R. (2014) *FgSKN7* and *FgATF1* have overlapping functions in ascosporogenesis, pathogenesis, and stress responses in *Fusarium graminearum*. *Environ. Microbiol.* 10.1111/1462-2920.12561
13. Guo, M., Guo, W., Chen, Y., Dong, S., Zhang, X., Zhang, H., Song, W., Wang, W., Wang, Q., Lv, R., Zhang, Z., Wang, Y., and Zheng, X. (2010) The basic leucine zipper transcription factor Moatf1 mediates oxidative stress responses and is necessary for full virulence of the rice blast fungus *Magnaporthe oryzae*. *Mol. Plant Microbe Interact.* **23,** 1053–1068
14. Guo, M., Chen, Y., Du, Y., Dong, Y., Guo, W., Zhai, S., Zhang, H., Dong, S., Zhang, Z., Wang, Y., Wang, P., and Zheng, X. (2011) The bZIP transcription factor MoAP1 mediates the oxidative stress response and is critical for pathogenicity of the rice blast fungus *Magnaporthe oryzae*. *PLoS Pathog.* **7,** e1001302
15. Tang, W., Ru, Y., Hong, L., Zhu, Q., Zuo, R., Guo, X., Wang, J., Zhang, H., Zheng, X., Wang, P., and Zhang, Z. (2014) System-wide characterization of bZIP transcription factor proteins involved in infection-related morphogenesis of *Magnaporthe oryzae*. *Environ. Microbiol.* 10.1111/1462-2920.12618
16. Gao, Q., Jin, K., Ying, S. H., Zhang, Y., Xiao, G., Shang, Y., Duan, Z., Hu, X., Xie, X. Q., Zhou, G., Peng, G., Luo, Z., Huang, W., Wang, B., Fang, W., Wang, S., Zhong, Y., Ma, L. J., St. Leger, R. J., Zhao, G. P., Pei, Y., Feng, M. G., Xia, Y., and Wang, C. (2011) Genome sequencing and comparative transcriptomics of the model entomopathogenic fungi *Metarhizium anisopliae* and *M. acridum*. *PLoS Genet.* **7,** e1001264
17. Zheng, P., Xia, Y., Xiao, G., Xiong, C., Hu, X., Zhang, S., Zheng, H., Huang, Y., Zhou, Y., Wang, S., Zhao, G. P., Liu, X., St. Leger, R. J., and Wang, C. (2011) Genome sequence of the insect pathogenic fungus *Cordyceps militaris*, a valued traditional Chinese medicine. *Genome Biol.* **12,** R116
18. Xiao, G., Ying, S. H., Zheng, P., Wang, Z. L., Zhang, S., Xie, X. Q., Shang, Y., St. Leger, R. J., Zhao, G. P., Wang, C., and Feng, M. G. (2012) Genomic perspectives on the evolution of fungal entomopathogenicity in *Beauveria bassiana*. *Sci. Rep.* **2,** 483
19. Hu, X., Xiao, G., Zheng, P., Shang, Y., Su, Y., Zhang, X., Liu, X., Zhan, S., St. Leger, R. J., and Wang, C. (2014) Trajectory and genomic determinants of fungal-pathogen speciation and host adaptation. *Proc. Natl. Acad. Sci. U.S.A.* **111,** 16796–16801
20. de Faria, M. R., and Wraight, S. P. (2007) Mycoinsecticides and mycoacaricides: a comprehensive list with worldwide coverage and international classification of formulation types. *Biol. Control* **43,** 237–256
21. Wang, C., and Feng, M. G. (2014) Advances in fundamental and applied studies in China of fungal biocontrol agents for use against arthropod pests. *Biol. Control* **68,** 129–135
22. St. Leger, R. J., and Wang, C. (2010) Genetic engineering of fungal biocontrol agents to achieve greater efficacy against insect pests. *Appl. Microbiol. Biotechnol.* **85,** 901–907
23. Boomsma, J. J., Jensen, A. B., Meyling, N. V., and Eilenberg, J. (2014) Evolutionary interaction networks of insect pathogenic fungi. *Annu Rev. Entomol.* **59,** 467–485
24. Duan, Z., Chen, Y., Huang, W., Shang, Y., Chen, P., and Wang, C. (2013) Linkage of autophagy to fungal development, lipid storage and virulence in *Metarhizium robertsii*. *Autophagy* **9,** 538–549
25. Wanchoo, A., Lewis, M. W., and Keyhani, N. O. (2009) Lectin mapping reveals stage-specific display of surface carbohydrates in *in vitro* and haemolymph-derived cells of the entomopathogenic fungus *Beauveria bassiana*. *Microbiology* **155,** 3121–3133
26. Zhang, S., Xia, Y. X., Kim, B., and Keyhani, N. O. (2011) Two hydrophobins are involved in fungal spore coat rodlet layer assembly and each play distinct roles in surface interactions, development and pathogenesis in the entomopathogenic fungus, *Beauveria bassiana*. *Mol. Microbiol.* **80,** 811–826
27. Wang, C., Typas, M. A., and Butt, T. M. (2002) Detection and characterisation of pr1 virulent gene deficiencies in the insect pathogenic fungus *Metarhizium anisopliae*. *FEMS Microbiol. Lett.* **213,** 251–255
28. Wang, C., Skrobek, A., and Butt, T. M. (2004) Investigations on the destruxin production of the entomopathogenic fungus *Metarhizium anisopliae*. *J. Invertebr. Pathol.* **85,** 168–174
29. Wang, J. C., Xu, H., Zhu, Y., Liu, Q. Q., and Cai, X. L. (2013) OsbZIP58, a basic leucine zipper transcription factor, regulates starch biosynthesis in rice endosperm. *J. Exp. Bot.* **64,** 3453–3466
30. Larkin, M. A., Blackshields, G., Brown, N. P., Chenna, R., McGettigan, P. A., McWilliam, H., Valentin, F., Wallace, I. M., Wilm, A., Lopez, R., Thompson, J. D., Gibson, T. J., and Higgins, D. G. (2007) ClustalW and ClustalX version 2.0. *Bioinformatics* **23,** 2947–2948
31. Tamura, K., Stecher, G., Peterson, D., Filipski, A., and Kumar, S. (2013) MEGA6: molecular evolutionary genetics analysis version 6.0. *Mol. Biol. Evol.* **30,** 2725–2729
32. Huang, W., Shang, Y., Chen, P., Gao, Q., and Wang, C. (2014) MrpacC regulates sporulation, insect cuticle penetration and immune evasion in *Metarhizium robertsii*. *Environ. Microbiol.* 10.1111/1462-2920.12451
33. Duan, Z., Shang, Y., Gao, Q., Zheng, P., and Wang, C. (2009) A phosphoketolase Mpk1 of bacterial origin is adaptively required for full virulence in the insect-pathogenic fungus *Metarhizium anisopliae*. *Environ. Microbiol.* **11,** 2351–2360
34. Gao, Q., Shang, Y., Huang, W., and Wang, C. (2013) Glycerol-3-phosphate acyltransferase contributes to triacylglycerol biosynthesis, lipid droplet formation, and host invasion in *Metarhizium robertsii*. *Appl. Environ. Microbiol.* **79,** 7646–7653
35. Selvaggini, S., Munro, C. A., Paschoud, S., Sanglard, D., and Gow, N. A. (2004) Independent regulation of chitin synthase and chitinase activity in *Candida albicans* and *Saccharomyces cerevisiae*. *Microbiology* **150,** 921–928
36. Yago, J. I., Lin, C. H., and Chung, K. R. (2011) The SLT2 mitogen-activated protein kinase-mediated signalling pathway governs conidiation, morphogenesis, fungal virulence and production of toxin and melanin in the tangerine pathotype of *Alternaria alternata*. *Mol. Plant Pathol.* **12,** 653–665
37. Wang, B., Kang, Q., Lu, Y., Bai, L., and Wang, C. (2012) Unveiling the biosynthetic puzzle of destruxins in *Metarhizium* species. *Proc. Natl. Acad. Sci. U.S.A.* **109,** 1287–1292
38. St. Leger, R. J., Bidochka, M. J., and Roberts, D. W. (1994) Isoforms of the cuticle-degrading Pr1 proteinase and production of a metalloproteinase by *Metarhizium anisopliae*. *Arch. Biochem. Biophys.* **313,** 1–7
39. Lu, D., Pava-Ripoll, M., Li, Z., and Wang, C. (2008) Insecticidal evaluation of *Beauveria bassiana* engineered to express a scorpion neurotoxin and a cuticle degrading protease. *Appl. Microbiol. Biotechnol.* **81,** 515–522
40. Chen, Y., Feng, P., Shang, Y., Xu, Y.J., and Wang, C. (2014) Biosynthesis of non-melanin pigment by a divergent polyketide synthase in *Metarhizium robertsii*. *Fungal Genet. Biol.* 10.1016/j.fgb.2014.10.018
41. Spode, I., Maiwald, D., Hollenberg, C. P., Suckow, M. (2002) ATF/CREB sites present in sub-telomeric regions of *Saccharomyces cerevisiae* chromosomes are part of promoters and act as UAS/URS of highly conserved *COS* genes. *J. Mol. Biol.* **319,** 407–420

42. Wang, C., Hu, G., and St. Leger, R. J. (2005) Differential gene expression by *Metarhizium anisopliae* growing in root exudate and host (*Manduca sexta*) cuticle or hemolymph reveals mechanisms of physiological adaptation. *Fungal Genet. Biol.* **42,** 704–718
43. Emri, T., Molnár, Z., Szilágyi, M., and Pócsi, I. (2008) Regulation of autolysis in *Aspergillus nidulans*. *Appl. Biochem. Biotechnol.* **151,** 211–220
44. Orlean, P. (1997) Biogenesis of yeast wall and surface components. *Cold Spring Harb. Monograph Arch.* **21,** 229–362
45. Lagorce, A., Le Berre-Anton, V., Aguilar-Uscanga, B., Martin-Yken, H., Dagkessamanskaia, A., and François, J. (2002) Involvement of *GFA1*, which encodes glutamine-fructose-6-phosphate amidotransferase, in the activation of the chitin synthesis pathway in response to cell-wall defects in *Saccharomyces cerevisiae*. *Eur. J. Biochem.* **269,** 1697–1707
46. Wang, C., and St. Leger, R. J. (2007) The MAD1 adhesin of *Metarhizium anisopliae* links adhesion with blastospore production and virulence to insects, and the MAD2 adhesin enables attachment to plants. *Eukaryot. Cell* **6,** 808–816
47. Conkright, M. D., Guzmán, E., Flechner, L., Su, A. I., Hogenesch, J. B., Montminy, M. (2003) Genome-wide analysis of CREB target genes reveals a core promoter requirement for cAMP responsiveness. *Mol. Cell* **11,** 1101–1108
48. Gabaldón, T., and Koonin, E. V. (2013) Functional and evolutionary implications of gene orthology. *Nat. Rev. Genet.* **14,** 360–366
49. Zheng, P., Xia, Y., Zhang, S., and Wang, C. (2013) Genetics of *Cordyceps* and related fungi. *Appl. Microbiol. Biotechnol.* **97,** 2797–2804
50. Ramana, K. V., Kandi, S., Bharatkumar, V., Sharada, C. V., Rao, R., Mani, R., and Rao, S. D. (2013) Invasive fungal infections: a comprehensive review. *Am. J. Infect. Dis. Microbiol.* **1,** 64–69
51. Ragni, E., Fontaine, T., Gissi, C., Latgè, J. P., and Popolo, L. (2007) The Gas family of proteins of *Saccharomyces cerevisiae*: characterization and evolutionary analysis. *Yeast* **24,** 297–308
52. Alberti-Segui, C., Morales, A. J., Xing, H., Kessler, M. M., Willins, D. A., Weinstock, K. G., Cottarel, G., Fechtel, K., and Rogers, B. (2004) Identification of potential cell-surface proteins in *Candida albicans* and investigation of the role of a putative cell surface glycosidase in adhesion and virulence. *Yeast* **21,** 285–302
53. Calderon, J., Zavrel, M., Ragni, E., Fonzi, W. A., Rupp, S., and Popolo, L. (2010) *PHR1*, a pH-regulated gene of *Candida albicans* encoding a glucan-remodelling enzyme, is required for adhesion and invasion. *Microbiology* **156,** 2484–2494
54. Cabib, E., Farkas, V., Kosík, O., Blanco, N., Arroyo, J., and McPhie, P. (2008) Assembly of the yeast cell wall. Crh1p and Crh2p act as transglycosylases *in vivo* and *in vitro*. *J. Biol. Chem.* **283,** 29859–29872
55. St. Leger, R. J., Joshi, L., Bidochka, M. J., and Roberts, D. W. (1996) Construction of an improved mycoinsecticide overexpressing a toxic protease. *Proc. Natl. Acad. Sci. U.S.A.* **93,** 6349–6354
56. Chen, L., Zou, G., Zhang, L., de Vries, R. P., Yan, X., Zhang, J., Liu, R., Wang, C., Qu, Y., and Zhou, Z. (2014) The distinctive regulatory roles of PrtT in the cell metabolism of *Penicillium oxalicum*. *Fungal Genet. Biol.* **63,** 42–54